ChemComm

COMMUNICATION

View Article Online
View Journal | View Issue

Cite this: *Chem. Commun.*, 2015, **51**, 14501

Received 28th May 2015,
Accepted 6th August 2015

DOI: 10.1039/c5cc04365d

www.rsc.org/chemcomm

Light-responsive peptide [2]rotaxanes as gatekeepers of mechanised nanocontainers†

A. Martinez-Cuezva, S. Valero-Moya, M. Alajarin and J. Berna*

Novel mechanized silica nanoparticles incorporating a peptide-based molecular shuttle as a photo-responsive interlocked gatekeeper of nanocontainers are described including the uptake and delivery studies of a model cargo.

Since the beginning of this century the use of mesoporous materials for the smart delivery of cargoes has been an appealing research topic.[1,2] In these studies systems devoted to the controlled release of drugs have a singular significance due to their promising therapeutic use.[3] In this arena, mesoporous silica nanoparticles (MSNs) have become outstanding materials for controlled delivery applications due to their exceptional features such as high loading capacity, wide diversity regarding size, shape and pore diameter, easy functionalization, mechanical and chemical resistance and biocompatibility.[4,5] Numerous stimuli-responsive methods[6] have been established to govern the trapping and liberation of small molecules from the pores of these nanocontainers incorporating different organic or inorganic motifs behaving as blockers or gatekeepers. One promising group of these tailor-made doors is based on threaded/interlocked structures,[7] giving rise to the materials known as mechanized silica nanoparticles[8] which have been seen as intelligent materials with excellent potential for the advancement of novel nanodosifiers.[9] Typically, the benefits of the MSNs and the well-known templating method to assemble MCM-41 make this silica support the preferred choice for probing the ability of [2]pseudorotaxanes or bistable [2]rotaxanes to act as controllable gates of their pores. In this regard, a variety of mechanized silica having different macrocyclic components, including cyclophanes,[10] crown ethers,[11] cucurbiturils[12] and cyclodextrins,[13] as gatekeepers of these nanocontainers, has been investigated. To the best of our knowledge, the positional switching of benzylic amide rings has never been tested as an open/close mechanism for controlling the release and capture of cargoes from MSNs.

Among the [2]rotaxanes containing a benzylic amide macrocycle pioneered by Leigh,[7b–e] the subset of the peptide-based structures[14–17] are considered excellent scaffolds for the building of a broad range of molecular shuttles,[14] logic gates,[15] information storage devices[16] and enzymatic delivery systems of bioactive compounds.[17]

Herein, we describe the preparation of novel mechanized silica nanoparticles having a peptide-based molecular shuttle as a photocontrollable gatekeeper and MCM-41 as a mesoporous support aimed at the construction of light-operated nanocontainers. The loading and delivery of rhodamine B (RhB) as a model cargo through the mechanism depicted in Fig. 1 have also been reported.

Our system is based on the light-induced *E*/*Z* isomerization of a fumaramide-based binding site for shuttling the macrocycle along the thread of a bistable [2]rotaxane[18] thus closing and opening a molecular gate on the surface of a mesoporous silica support. We placed a peptide station (green cylinder, Fig. 1a) near the silica surface and connected to a fumaramide station (red cylinder) by an alkyl chain. In the open-pore state, the tetralactame ring is located on the fumaramide station allowing the free diffusion of the cargo RhB molecules (purple blocks) toward the void of the pores. The photoisomerization of the olefin affording the maleamide derivative (pink cylinder) alters the binding affinity of the unsaturated station by several kilocalories per mole[19] and promotes the ring translocation towards the peptide-based binding site for entrapping the cargo (Fig. 1a). A *cis*-to-*trans* olefin isomerization shuttles back the ring to the fumaramide station, thus opening the pores for enabling the release of the RhB molecules and allowing the reusability of these nanocontainers.

The matching of the porous mesostructure of the silica nanoparticles (*ca.* 100–200 nm diameter) containing hexagonally arranged pores (*ca.* 2 nm diameter) and the relative sizes[20] of the model cargo (RhB: 1.0 × 1.5 nm) and the ring (benzylic tetralactame: 0.8 × 1.7 nm) supports the ability of the latter for

Departamento de Química Orgánica, Facultad de Química, Regional Campus of International Excellence "Campus Mare Nostrum", Universidad de Murcia, E-30100, Murcia, Spain. E-mail: ppberna@um.es

† Electronic supplementary information (ESI) available: Synthetic procedures, experimental details and characterization. See DOI: 10.1039/c5cc04365d

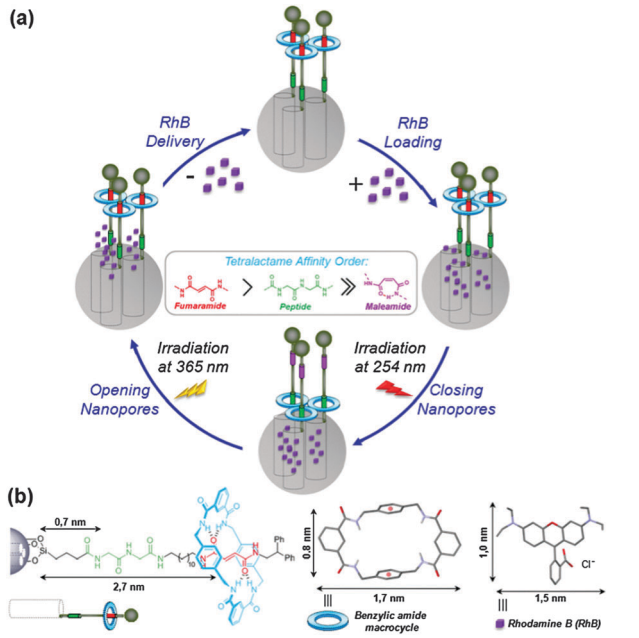

Fig. 1 (a) Uptake and release of dye cargo molecules (RhB) from the pores of a MCM-41 silica functionalized with a light-responsive peptide [2]rotaxane. The movable lid is a tetralactame which locates on the preferred station (fumaramide, red cylinder, or peptide, green cylinder) depending on its affinity order. (b) Relative distance of the silicon atom to the first HB acceptor of the stations that are connected by the thread, illustrating the feasibility of the RhB loading. Cross dimensions (in nm) of the sealing tetralactame (blue ring) and the RhB cargo molecule (purple block) showing up the size matching with the average diameter (*ca.* 2 nm) of nanopores of the silica support. Molecular modeling structures of the macrocycle and the RhB cation are shown. Distances values were obtained from the CCDC database (see ref. 20).

keeping the cargo molecules inside the pores (Fig. 1b). In addition, the relative distance of each station of the [2]rotaxane with respect to the porous surface regulates the position of the moveable lid and, consequently, it determines the limiting cross-dimensions of the loading cargo molecules to be longer than 0.7 nm but shorter than 2.7 nm.

Tetraethylorthosilicate as the silicon source and cetyltrimethylammonium bromide (CTAB) as the template were used in a base-catalyzed sol–gel protocol[21] for affording the mesostructured silica of the MCM-41 type (**MSN-1**). The size and the mesoporous structure of the nanoparticles were studied by scanning electron and transmission electron microscopy, respectively (see Fig. S1a and b, ESI†).

The final **MSN-*E*-6** system was assembled in a stepwise synthesis from the thermoactivated[22] silica nanoparticles (Scheme 1). First, the spherical surface of **MSN-1** was functionalized with nitrile functions affording **MSN-2** by heating with 2-cyanoethyltriethoxysilane in toluene. Further refluxing with 50% sulfuric acid provided the surface-bound carboxylic acid **MSN-3**. Next, amide bond formation between the carboxy groups of **MSN-3** with the glycylglycine building block **S1** (see the ESI†) in the presence of *N*,*N*-dicyclohexylcarbodiimide afforded the corresponding phthalimide-functionalized particles **MSN-4**. Subsequent hydrazinolysis[23] of the preceding silica provided the amino-functionalized **MSN-5** which was completely separated from the phthalhydrazide byproduct by

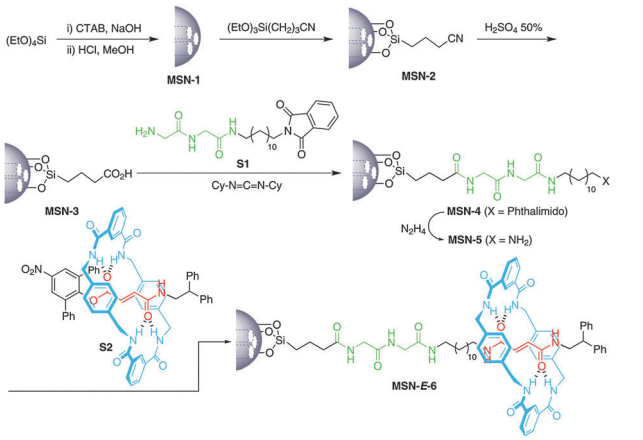

Scheme 1 Synthesis of the mesoporous silica nanoparticles **MSN-*E*-6** functionalized with a photocontrollable peptide [2]rotaxane.

continuous extraction in a Soxhlet apparatus with hot ethanol. Finally, the nucleophilic substitution of the bulky 2,6-diphenyl-4-nitrophenoxy stopper[17a] of the fumaramide rotaxane **S2** (see the ESI†) by the amino groups of the latter silica particles yielded the target **MSN-*E*-6** with a surface gated with a two-station peptide [2]rotaxane (Scheme 1).

Non-mechanized nanoparticles **MSN-7** bearing an identical linear fragment to that of **MSN-*E*-6** were also prepared according to the synthetic route outlined in Scheme 2. In this regard, the amine **2** was prepared through a two consecutive amide coupling-Boc deprotection protocol for incorporating the fumaramide and peptide binding sites tethered by a dodecyl alkyl chain. Next, the carbodiimide-mediated amide formation between the acid-terminated surface of **MSN-3** and the amine **2** led to silica nanoparticles **MSN-7** which were used as non-threaded model materials, lacking the benzylic amide macrocycle.

The structure determination and characterization of the compounds and materials shown in the Schemes 1 and 2 were accomplished by means of their analytical and spectral data (see the ESI†). Although intense bands of the Si–O–Si stretching and bending vibrations at 1080 and 800 cm^{-1} are present in the FTIR spectra of all the silica materials shown in these schemes (see Fig. S3 and S4, ESI†) the functional groups incorporated in each stage are also evidenced in these spectra. Thus, the spectrum of **MSN-3** shows a weak band at 2953 cm^{-1} owing to the C–H stretching and a strong one at 1726 cm^{-1} corresponding to the C=O stretching vibration of

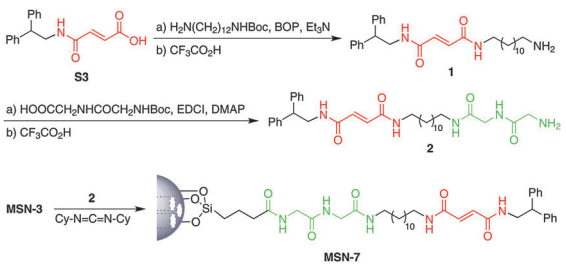

Scheme 2 Synthesis of the mesoporous silica nanoparticles **MSN-7** functionalized with the two-binding site thread precursor **2**.

the carboxy group. At the end of the transformations outlined in Scheme 1, the FTIR spectrum of the interlocked **MSN-*E*-6** shows two intense C═O bands at 1646 and 1540 cm^{-1} corresponding to the C═O stretching vibrations of the different amido groups of the gatekeeper, also displaying intense bands in the range of 2983 and 2894 cm^{-1} due to the methylene groups present in this motif. ^{29}Si and ^{13}C cross-polarization magic-angle spinning solid-state (SS) NMR spectroscopies were also used to examine the grafting and attachment of the different organic fragments into MCM-41. The ^{29}Si SSNMR spectrum (see Fig. S5, ESI†) of the silica **MSN-2** shows two T signals at −54.8 and −61.9 ppm corresponding to the silicon atoms directly connected to the organic fragments and a Q signal at −109.5 ppm ascribed to the rest of silicon atoms [$Si(OSi)_n(OH)_{4-n}$; n = 2–4]. The measurement of the ^{13}C SSNMR spectrum of each of the new synthesized material confirmed the successive chemical transformations toward the final mechanized silica (see the ESI†). The spectrum of the targeted **MSN-*E*-6** shows several sets of signals at different chemical shift ranges: at 174.1–163.3 ppm appear those corresponding to the carbon atoms of the carbonyl groups of the amide functions, at 144.8–116.4 ppm those of the aromatic carbon atoms and in the region between 70 and 10 ppm come out those of the aliphatic carbon atoms (see Fig. S7, ESI†). The comparison of this ^{13}C SSNMR spectra with the one of the non-interlocked **MSN-7** materials displays noticeable differences evidencing the lack of the tetralactame in this latter material (see Fig. S7, ESI†) further proving the functionalization of **MSN-*E*-6**. Finally, TGA and elemental analysis showed the rough estimation of the maximum amount of these interlocked motifs on the surface of **MSN-*E*-6** to be approximately 0.30 mmol per gram of silica.

Next the light-responsive gating behavior of **MSN-*E*-6** was investigated. The diffusion of the RhB cargo into the pores of this light-responsive silica was carried out by soaking the mechanized nanoparticles in a stirred aqueous solution of the guest compound for 24 h. The surface-adsorbed excess of the cargo was thoroughly washed and the resulting material was carefully dried. Then the pores of the material were sealed by means of a *trans*-to-*cis* photoisomerization of the olefin station[14c,18,24] by irradiation at 254 nm promoting the shifting of the tetralactame ring toward the peptide station close to the surface of the nanoparticulate silica. This operation kinetically entraps the guest molecules into the **MSN-*Z*-6** container and, then, the RhB loaded silica is thoroughly washed and dried. Although the accessibility of the cargo to the pores of **MSN-1** decreased after its functionalization with the rotaxane, as it was confirmed by the TEM observation (see Fig. S14, ESI†); the openings of the gated material still permitted the entrance of enough RhB for carrying out the study of its controlled release.

The delivery of RhB from the nanopores of **MSN-*Z*-6** was investigated in two different solvents, dichloromethane and water. For closely related interlocked systems[18] it is known that the polarity of the solvent affects the position of the ring over the peptide binding site. Thus, whereas in non-disrupting hydrogen bond solvents such as dichloromethane the ring is mainly located on the peptide station, in polar solvents the alkyl chain would act as a second solvophobic station.[18] For this purpose, a stirred suspension of RhB-loaded **MSN-*Z*-6** was irradiated at 365 nm for promoting the *cis*-to-*trans* isomerization which triggers the ring translocation to the most energetically favorable binding site that, in this case, is the resulting fumaramide station far away from the surface of the nanoparticulate silica. Consequently, this latter irradiation promotes the opening of the pores and the release of RhB, which was monitored by measuring the absorbance spectrum at different times (Fig. 2, inset). The obtained profile for the light-driven opening of the gatekeepers of this silica in dichloromethane shows a progressive delivery of the cargo reaching 50% of the maximum delivery in 50 min and needing 30 min more to reach a liberation of 80% of the cargo (Fig. 2a). Using Beer–Lambert's law, the RhB loading was calculated revealing that, for 3 mg of RhB-loaded **MSN-*Z*-6**, 0.175 μmol (2.8 wt%) of the cargo was released (see ESI†).

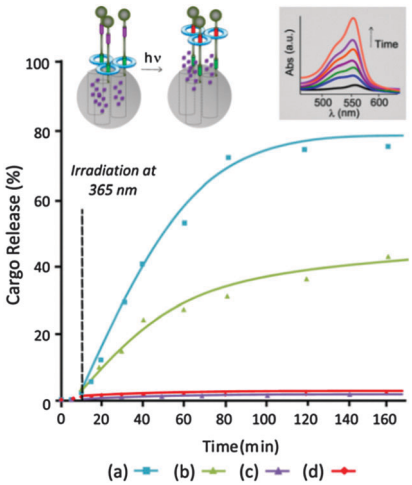

Fig. 2 Comparison of the release profiles of RhB from **MSN-*Z*-6** in dichloromethane solution (a and c) and aqueous solution (b and d). These experiments were carried out at 25 °C under light irradiation at 365 nm (a and b) and without photoactivation (c and d). The inset displays the absorption spectral change at 553 nm after the irradiation with 365 nm light of a suspension of RhB-loaded **MSN-*Z*-6**.

When the release experiment was carried out in water, the discharge of half the load lasted 200 min and the release profile of the rest is extended for more than 5 h (Fig. 2b). Consequently the remarkable positional integrity of the ring after photoisomerization of the maleamide binding site to its *trans* isomer promotes the expected release of the cargo in dichloromethane, and less quickly in water due to the decrease of the ring discrimination. At this point it is convenient to remark that slow dynamics release profiles as that shown in Fig. 2b are desirable in therapeutic treatments as they allow a moderated liberation of potent (and/or short half-life) drugs.[2,3]

It should also be noted that the interlocked nanogates of this container prevent significant premature release of the cargo dye molecules as revealed by the flat region (0–10 min) of the profiles in both solvents (Fig. 2a and b). We also carried out control experiments by monitoring the absorbance of RhB-loaded **MSN-*Z*-6** in the absence of light in both studied solvents (Fig. 2c and d), showing the absence of leaking processes under such conditions. Incidentally, these latter results also give an idea of the positional integrity of the ring over the peptide-based binding site in **MSN-*Z*-6** (see ESI†). Release control experiments with the non-mechanized material RhB-loaded **MSN-7** disclosed

a quick leaking of the guest molecules into solution confirming the key role of the benzylic amide macrocycle as the interlocked gatekeeper of **MSN-6** (see ESI†).

In summary, we have demonstrated the feasibility of building mechanized silica nanoparticles using a peptide-based molecular shuttle and MCM-41 as a mesoporous support. We have shown the efficiency of this particular functionalization in actuating as gatekeepers upon exposure to visible light irradiation displaying different dosages depending on the working conditions. The unprecedented integration of a benzylic tetralactame as a movable lid allows a proficient uptake and release of RhB employed as the model cargo. This mechanized material must be included in the yet scarce number of described light-operated molecular nanovalves and opens stimulating opportunities for the development of a novel generation of smart nanocontainers by anchoring amide-based interlocked compounds, which could be used as controlled delivery systems.

This work was supported by the MINECO (CTQ2009-12216/BQU and CTQ2014-56887-P) and the Fundacion Seneca-CARM (Project 19240/PI/14). A.M.-C. thanks the Marie Curie COFUND/U-IMPACT programs and the MINECO for postdoctoral contracts. We also thank Prof. José M. González and Dr Almudena Torres of the National Center for Electron Microscopy (UCM, Madrid) for their helpful assistance with the TEM observations.

Notes and references

1 *Organic Nanomaterials*, ed. T. Torres and G. Bottari, Wiley, Hoboken, US2013.
2 (*a*) A. P. Wight and M. E. Davis, *Chem. Rev.*, 2002, **102**, 3589–3613; (*b*) L. Nicole, C. Laberty-Robert, L. Rozes and C. Sanchez, *Nanoscale*, 2014, **6**, 6267–6292; (*c*) N. Linares, A. M. Silvestre-Albero, E. Serrano, J. Silvestre-Albero and J. Garcia-Martinez, *Chem. Soc. Rev.*, 2014, **43**, 7681–7717; (*d*) S. Alberti, G. J. A. A. Soler-Illia and O. Azzaroni, *Chem. Commun.*, 2015, **51**, 6050–6075.
3 (*a*) M. Vallet-Regi, F. Balas and D. Arcos, *Angew. Chem., Int. Ed.*, 2007, **46**, 7548–7558; (*b*) M. Vallet-Regi, M. Colilla and B. Gonzalez, *Chem. Soc. Rev.*, 2011, **40**, 596–607; (*c*) M. Colilla and M. Vallet-Regi, *Smart Mater. Drug Deliv.*, 2013, **2**, 63–89.
4 (*a*) C. Argyo, V. Weiss, C. Bräuchle and T. Bein, *Chem. Mater.*, 2014, **26**, 435–451; (*b*) A. Baeza, M. Colilla and M. Vallet-Regi, *Expert Opin. Drug Delivery*, 2015, **12**, 319–337.
5 For some recent studies of biocompatible MSNs with exceptional cargo delivery properties see: (*a*) S. R. Gayam and S.-P. Wu, *J. Mater. Chem. B*, 2014, **2**, 7009–7016; (*b*) P. Pakawanit, S. Ananta, T. K. Yun, J. Y. Bae, W. Jang, H. Byun and J.-H. Kim, *RSC Adv.*, 2014, **4**, 39287–39296; (*c*) Y.-J. Cheng, G.-F. Luo, J.-Y. Zhu, X.-D. Xu, X. Zeng, D.-B. Cheng, Y.-M. Li, Y. Wu, X.-Z. Zhang, R.-X. Zhuo and F. He, *ACS Appl. Mater. Interfaces*, 2015, **7**, 9078–9087.
6 (*a*) B. G. Trewyn, I. I. Slowing, S. Giri, H.-T. Chen and V. S.-Y. Lin, *Acc. Chem. Res.*, 2007, **40**, 846–853; (*b*) E. Aznar, R. Martinez-Mañez and F. Sancenon, *Expert Opin. Drug Delivery*, 2009, **6**, 643–655; (*c*) C. Coll, A. Bernardos, R. Martinez-Mañez and F. Sancenon, *Acc. Chem. Res.*, 2013, **46**, 339–349.
7 (*a*) D. B. Amabilino and J. F. Stoddart, *Chem. Rev.*, 1995, **95**, 2725–2829; (*b*) E. R. Kay, D. A. Leigh and F. Zerbetto, *Angew. Chem., Int. Ed.*, 2007, **46**, 72–191; (*c*) W. Yang, Y. Li, H. Liu, L. Chi and Y. Li, *Small*, 2012, **8**, 504–516; (*d*) M. Xue, Y. Yang, X. Chi, X. Yan and F. Huang, *Chem. Rev.*, 2015, **115**, 7398–7501; (*e*) D.-H. Qu, Q.-C. Wang, Q.-W. Zhang, X. Ma and H. Tian, *Chem. Rev.*, 2015, **115**, 7543–7588.
8 (*a*) K. K. Coti, M. E. Belowich, M. Liong, M. W. Ambrogio, Y. A. Lau, H. A. Khatib, J. I. Zink, N. M. Khashab and J. F. Stoddart, *Nanoscale*, 2009, **1**, 16–39; (*b*) M. W. Ambrogio, C. R. Thomas, Y.-L. Zhao, J. I. Zink and J. F. Stoddart, *Acc. Chem. Res.*, 2011, **44**, 903–913; (*c*) Y. W. Yang, Y. L. Sun and N. Song, *Acc. Chem. Res.*, 2014, **47**, 1950–1960.
9 (*a*) C. Y. Ang, S. Y. Tan and Y. Zhao, *Org. Biomol. Chem.*, 2014, **12**, 4776–4806; (*b*) X. Ma and Y. Zhao, *Chem. Rev.*, 2015, **115**, 7794–7839.
10 (*a*) R. Hernandez, H. R. Tseng, J. W. Wong, J. F. Stoddart and J. I. Zink, *J. Am. Chem. Soc.*, 2004, **126**, 3370–3371; (*b*) T. D. Nguyen, H.-R. Tseng, P. C. Celestre, A. H. Flood, Y. Liu, J. F. Stoddart and J. I. Zink, *Proc. Natl. Acad. Sci. U. S. A.*, 2005, **102**, 10029–10034.
11 (*a*) T. D. Nguyen, K. C.-F. Leung, M. Liong, C. D. Pentecost, J. F. Stoddart and J. I. Zink, *Org. Lett.*, 2006, **8**, 3363–3366; (*b*) T. D. Nguyen, Y. Liu, S. Saha, K. C.-F. Leung, J. F. Stoddart and J. I. Zink, *J. Am. Chem. Soc.*, 2007, **129**, 626–634.
12 For examples containing CB[6] rings see: (*a*) C. R. Thomas, D. P. Ferris, J.-H. Lee, E. Choi, M. H. Cho, E. S. Kim, J. F. Stoddart, J.-S. Shin, J. Cheon and J. I. Zink, *J. Am. Chem. Soc.*, 2010, **132**, 10623–10625; (*b*) M. Wang, T. Chen, C. Ding and J. Fu, *Chem. Commun.*, 2014, **50**, 5068–5071. For recent examples containing CB[7] rings see: (*c*) Y. L. Sun, B. J. Yang, S. X. A. Zhang and Y. W. Yang, *Chem. – Eur. J.*, 2012, **18**, 9212–9216; (*d*) J. Fu, T. Chen, M. Wang, N. Yang, S. Li, Y. Wang and X. Liu, *ACS Nano*, 2013, **7**, 11397–11408. For a recent example containing CB[8] rings see: (*e*) C. Hu, Y. Lan, F. Tian, K. R. West and O. A. Scherman, *Langmuir*, 2014, **30**, 10926–10932.
13 For recent examples containing α-CD rings see: (*a*) Z. Luo, X. Ding, Y. Hu, S. Wu, Y. Xiang, Y. Zeng, B. Zhang, H. Yan, H. Zhang, L. Zhu, J. Liu, J. Li, K. Cai and Y. Zhao, *ACS Nano*, 2013, **7**, 10271–10284; (*b*) D. Tarn, D. P. Ferris, J. C. Barnes, M. W. Ambrogio, J. F. Stoddart and J. I. Zink, *Nanoscale*, 2014, **6**, 3335–3343. For some examples containing β-CD rings see: (*c*) Y.-L. Zhao, Z. Li, S. Kabehie, Y. Y. Botros, J. F. Stoddart and J. I. Zink, *J. Am. Chem. Soc.*, 2010, **132**, 13016–13025; (*d*) C. Wang, Z. Li, D. Cao, Y.-L. Zhao, J. W. Gaines, O. A. Bozdemir, M. W. Ambrogio, M. Frasconi, Y. Y. Botros, J. I. Zink and J. F. Stoddart, *Angew. Chem., Int. Ed.*, 2012, **51**, 5460–5465; (*e*) M. D. Yilmaz, M. Xue, M. W. Ambrogio, O. Buyukcakir, Y. Wu, M. Frasconi, X. Chen, M. S. Nassar, J. F. Stoddart and J. I. Zink, *Nanoscale*, 2015, **7**, 1067–1072.
14 (*a*) A. S. Lane, D. A. Leigh and A. Murphy, *J. Am. Chem. Soc.*, 1997, **119**, 11092–11093; (*b*) G. W. H. Wurpel, A. M. Brouwer, I. H. M. van Stokkum, A. Farran and D. A. Leigh, *J. Am. Chem. Soc.*, 2001, **123**, 11327–11328; (*c*) G. Bottari, D. A. Leigh and E. M. Perez, *J. Am. Chem. Soc.*, 2003, **125**, 13360–13361.
15 D. A. Leigh, M. A. F. Morales, E. M. Perez, J. K. Y. Wong, C. G. Saiz, A. M. Z. Slawin, A. J. Carmichael, D. M. Haddleton, A. M. Brouwer, W. J. Buma, G. W. H. Wurpel, S. Leon and F. Zerbetto, *Angew. Chem., Int. Ed.*, 2005, **44**, 3062–3067.
16 M. Cavallini, F. Biscarini, S. Leon, F. Zerbetto, G. Bottari and D. A. Leigh, *Science*, 2003, **299**, 531.
17 (*a*) A. Fernandes, A. Viterisi, F. Coutrot, S. Potok, D. A. Leigh, V. Aucagne and S. Papot, *Angew. Chem., Int. Ed.*, 2009, **48**, 6443–6447; (*b*) A. Fernandes, A. Viterisi, V. Aucagne, D. A. Leigh and S. Papot, *Chem. Commun.*, 2012, **48**, 2083–2085; (*c*) R. Barat, T. Legigan, I. Tranoy-Opalinski, B. Renoux, E. Péraudeau, J. Clarhaut, P. Poinot, A. E. Fernandes, V. Aucagne, D. A. Leigh and S. Papot, *Chem. Sci.*, 2015, **6**, 2608–2613.
18 E. M. Perez, D. T. F. Dryden, D. A. Leigh, G. Teobaldi and F. Zerbetto, *J. Am. Chem. Soc.*, 2004, **126**, 12210–12211.
19 (*a*) A. Altieri, G. Bottari, F. Dehez, D. A. Leigh, J. K. Y. Wong and F. Zerbetto, *Angew. Chem., Int. Ed.*, 2003, **42**, 2296–2300; (*b*) G. Bottari, F. Dehez, D. A. Leigh, P. J. Nash, E. M. Perez, J. K. Y. Wong and F. Zerbetto, *Angew. Chem., Int. Ed.*, 2003, **42**, 5886–5889.
20 These cross dimensions are average values resulting from the crystallographic distances of related structures included in the CCDC database, CSD 5.36 update Feb 2015.
21 S. Huh, J. W. Wiench, J.-C. Yoo, M. Pruski and V. S.-Y. Lin, *Chem. Mater.*, 2003, **15**, 4247–4256.
22 A. J. Butterworth, J. H. Clark, P. H. Walton and S. J. Barlow, *Chem. Commun.*, 1996, 1859–1860.
23 Preliminary studies revealed that the hydrazinolysis, in a number of reaction conditions (N_2H_4 or $MeNHNH_2$), of a closely related material to **MSN-4** but containing a GlyGly ester function as that incorporated in the reported molecular shuttle in ref. 18 resulted in a decomposition of the starting material instead of the exclusive expected amine formation.
24 P. Altoe, N. Haraszkiewicz, F. G. Gatti, P. G. Wiering, C. Frochot, A. M. Brouwer, G. Balkowski, D. Shaw, S. Woutersen, W. J. Buma, F. Zerbetto, G. Orlandi, D. A. Leigh and M. Garavelli, *J. Am. Chem. Soc.*, 2009, **131**, 104–117.

